ResearchGate

See discussions, stats, and author profiles for this publication at: https://www.researchgate.net/publication/267756755

Construction of a General Library for the Rational Design of Nanomagnets and Spin Qubits Based on Mononuclear f-Block Complexes. The Polyoxometalate Case

ARTICLE *in* INORGANIC CHEMISTRY · AUGUST 2014

Impact Factor: 4.76 · DOI: 10.1021/ic501867d · Source: PubMed

CITATIONS
9

READS
51

6 AUTHORS, INCLUDING:

Juan Modesto Clemente-Juan
University of Valencia
171 PUBLICATIONS **6,616** CITATIONS
SEE PROFILE

Eugenio Coronado
University of Valencia
610 PUBLICATIONS **18,956** CITATIONS
SEE PROFILE

Yan DUAN
University of Valencia
9 PUBLICATIONS **88** CITATIONS
SEE PROFILE

Alejandro Gaita-Ariño
University of Valencia
69 PUBLICATIONS **2,018** CITATIONS
SEE PROFILE

Available from: Yan DUAN
Retrieved on: 03 February 2016

Inorganic Chemistry

Article

pubs.acs.org/IC

Construction of a General Library for the Rational Design of Nanomagnets and Spin Qubits Based on Mononuclear f-Block Complexes. The Polyoxometalate Case

José J. Baldoví, Juan M. Clemente-Juan, Eugenio Coronado,* Yan Duan, Alejandro Gaita-Ariño,* and Carlos Giménez-Saiz

Instituto de Ciencia Molecular, Universidad de Valencia Catedrático José Beltrán no. 2, Paterna, Valencia 46980, Spain

Supporting Information

ABSTRACT: This paper belongs to a series of contributions aiming at establishing a general library that helps in the description of the crystal field (CF) effect of any ligand on the splitting of the J ground states of mononuclear f-element complexes. Here, the effective parameters associated with the oxo ligands (effective charges and metal−ligand distances) are extracted from the study of the magnetic properties of the first two families of single-ion magnets based on lanthanoid polyoxometalates (POMs), formulated as $[Ln(W_5O_{18})_2]^{9-}$ and $[Ln(\beta_2\text{-}SiW_{11}O_{39})_2]^{13-}$ (Ln = Tb, Dy, Ho, Er, Tm, Yb). This effective CF approach provides a good description of the lowest-lying magnetic levels and the associated wave functions of the studied systems, which is fully consistent with the observed magnetic behavior. In order to demonstrate the predictive character of this model, we have extended our model in a first step to calculate the properties of the POM complexes of the early 4f-block metals. In doing so, $[Nd(W_5O_{18})_2]^{9-}$ has been identified as a suitable candidate to exhibit SMM behavior. Magnetic experiments have confirmed such a prediction, demonstrating the usefulness of this strategy for the directed synthesis of new nanomagnets. Thus, with an effective barrier of 51.4 cm^{-1} under an applied dc field of 1000 Oe, this is the second example of a Nd^{3+}-based single-ion magnet.

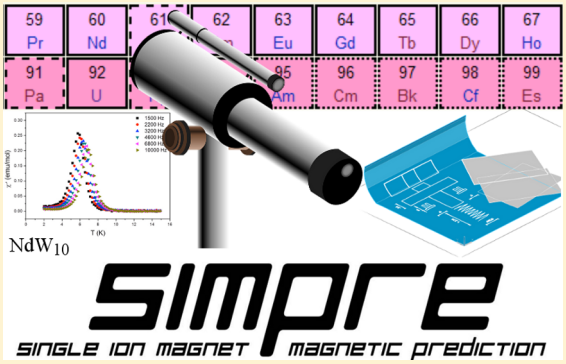

INTRODUCTION

Over the past decade, molecular magnetism has been rejuvenated with the discovery that some mononuclear f-element complexes display a single-molecule magnetic (SMM) behavior and novel quantum phenomena arising from their electronic structure.[1] These magnetic molecules, also known as single-ion magnets (SIMs), represent the limit of miniaturization of a nanomagnet, as they are based on a magnetically anisotropic single metal ion. The first example was reported by Ishikawa in the lanthanoid complexes of general formula $[LnPc_2]^-$, with phthalocyanines as ligands, displaying a square-antiprismatic coordination environment.[2] In view of the fact that polyoxometalate (POM) chemistry can also encapsulate lanthanoid complexes with D_{4d} symmetry, we decided to study the magnetic properties of the $[Ln(W_5O_{18})_2]^{9-}$ series (abbreviated LnW_{10}, where Ln = Tb (**1**), Dy (**2**), Ho (**3**), Er (**4**)), which became the second family of reported SIMs.[3] The best example with slow relaxation of the magnetization was the Er derivative, whereas in the Ishikawa series such behavior had been observed in $[TbPc_2]^-$. The reason for this difference was assumed to lie in the different distortion of the antiprismatic site, which is compressed in the second family (Er^{3+} is an oblate cation), instead of axially elongated in $[LnPc_2]^-$ (Tb^{3+} is a prolate cation).[4] The experimental studies of the first series of POM-based SIMs were extended to the $[Ln(ß_2\text{-}SiW_{11}O_{39})_2]^{13-}$ series (abbreviated LnW_{22}, where Ln = Tb (**5**), Dy (**6**), Ho (**7**), Er (**8**), Tm (**9**), Yb (**10**)),[5] which allowed the analysis of the effects produced by a more distorted antiprismatic site over the spin relaxation processes. As potentially nuclear spin free systems offering different rigid and highly symmetrical coordination environments, POMs are in a nearly unique position for the design of both SIMs and model spin 1/2 systems (spin qubits), minimizing decoherence and unwanted relaxation processes.[6,7]

In the past few years, the concept of SIMs has been extended to a large number of families of mononuclear d transition metal,[8] lanthanoid,[3,5,9] and uranium[10] complexes. In contrast with the classical polynuclear SMMs, whose properties are governed by exchange interactions, in SIMs magnetic exchange is usually irrelevant. Thus, the magnetic properties mainly depend on the electronic spectrum resulting from the crystal field (CF) splitting and secondarily on the hyperfine coupling. As a consequence, a fairly complex CF Hamiltonian (H_{CF}) must be properly defined and the determination of the CF parameters that describe the ligand field effects is crucial for a full theoretical description. However, this has been a challenge in the area of spectroscopy of lanthanide compounds for many

Received: August 4, 2014
Published: August 26, 2014

 © 2014 American Chemical Society dx.doi.org/10.1021/ic501867d | Inorg. Chem. 2014, 53, 9976−9980

decades, and it is still an open problem. Although ab initio methods have been broadly employed for this purpose in the field of molecular magnetism, the crystal field model is at present the only practical model to analyze and simulate the energy level data sets of lanthanide ions in crystal hosts at the accuracy level of ~10 cm^{-1}.[11] Surprisingly, ab initio calculations of energy levels and magnetic properties showing deviations on the order of 20% from experimental data are claimed to be "state-of-the-art" and "accurate"[12] and, sometimes, these disagreements are hidden in the Supporting Information.[13] These issues of the CASSCF calculations, among others, have recently been critically reviewed by Kögerler et al.[14]

On the other hand, despite the complexity of the interaction between the chemical environment and the 4f orbitals in rare earth systems, the representation of the CF Hamiltonian by a sum of single particle operators has proven to be successful, as may be noted from the number of phenomenological models existing in the literature concerning CF parameters.[15−19] These models are of worth, not only because they can be used for elucidative purposes and comparison with experiment but also because they allow the prediction of the full set of CF parameters, most of them inaccessible from the experiment. Among these models, the radial effective charge (REC) model uses two *semiempirical* parameters that describe each kind of ligand: a phenomenological effective charge and an effective metal−ligand distance to account for covalent effects. This model has proven to be suitable in the study of the effect of ligands that can be treated as spherical or that have the electron density of the donor atom pointing directly toward the metal.[20,21,10e,22] It is important to note that inexpensive correlations among molecular structures, CF parameters, and the electronic properties are an essential step to rationalize which conditions are favorable for the discovery of new derivatives with interesting optical[23] and magnetic properties.[4b]

Following this line, this article belongs to a set of contributions that aim to inexpensively model the effect of different kinds of donor atoms, gradually establishing a general library for further studies. The idea is to assign a *fingerprint* for each kind of donor atom by two or three parameters. In this paper, the effective parameters associated with the oxo ligand are extracted from the magnetic properties of the first two families of lanthanoid polyoxometalate-based SIMs. Such results are used in a further step to study the magnetic properties of other POMs that may have SMM properties. Following this last point, in this work we predict the SMM behavior of the derivative $[Nd(W_5O_{18})_2]^{9-}$ (**11**). This would not have been expected otherwise, as it is almost unprecedented: there is only one known Nd-based SIM.[24] After the directed synthesis of NdW_{10}, we were able to experimentally check and confirm our prediction.

RESULTS

Modeling the Properties of the Series $[Ln(W_5O_{18})_2]^{9-}$ and $[Ln(ß_2\text{-}SiW_{11}O_{39})_2]^{13-}$. In both series, a lanthanoid metal is encapsulated between two monolacunary polyoxometalate anions acting as tetradentate ligands in a square-antiprismatic environment around the Ln(III) center, with a near-D_{4d} symmetry (Figure 1). In the complex $[Ln(W_5O_{18})_2]^{9-}$ each anionic moiety is twisted 44−45° with respect to the other, whereas in $[Ln(ß_2\text{-}SiW_{11}O_{39})_2]^{13-}$ they possess a more pronounced distortion, with a rotation angle between the two moieties of about 41°. Distortions from the ideal D_{4d} symmetry are responsible for the mixing in the wave functions and

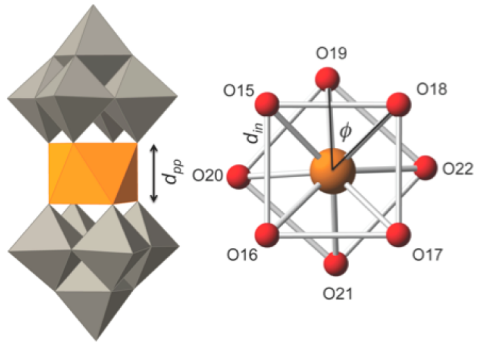

Figure 1. Molecular structure of $[Ln(W_5O_{18})_2]^{9-}$ (**1**−**4**) (left) and view of its square-antiprismatic coordination sphere (right). Complexes of the series $[Ln(ß_2\text{-}SiW_{11}O_{39})_2]^{13-}$ (**5**−**10**) have an isostructural coordination sphere.

generate non-negligible tunneling splitting in the non-Kramers derivatives. For example, a variation of only 3° in the twist angle means a difference of 1 order of magnitude between the HoW_{10} and HoW_{22} tunneling gaps.[25]

As we may observe in Figure 1, a well-defined magnetic axis is expected in the different derivatives because of the near-pseudoaxial symmetry of the compounds. Thus, in our calculations we have referred our coordinate system aligned with the main symmetry axis of the square antiprism. As the eight oxygen atoms are chemically equivalent, a simultaneous fit of the magnetic susceptibility data of **1**−**8** (available from ref 5) from 2 to 280 K has been performed. A satisfactory fitting of the χT product with only two REC parameters is obtained when D_r = 0.895 Å and Z_i = 0.105 with a relative error of $E = 3.56 \times 10^{-3}$. To test the validity of these two parameters, they have been applied to describe the magnetic properties of compounds **9** and **10**. As one can see, the agreement between the model and all of the experimental data is excellent (Figure 2), even for TmW_{22} and YbW_{22}, which were not included in the collective fit. Energy level schemes and ground-state descriptions of **1**−**4** (Figure S1) and **5**−**10** (Figure S2) are available as Supporting Information.

As an example, the energy level schemes and main contributions to the wave functions of compounds ErW_{10} (**4**) and YbW_{22} (**10**) are shown in Figure 3. One may observe the high contribution of a high M_J value in both cases (99% of ±13/2 and 97% of ±5/2 for **4** and **10**, respectively), which explains why both behave as SIMs exhibiting slow relaxation of the magnetization at low temperatures. Also, to explore the possibility of having more SIMs, we have used the above model to predict the properties in other lanthanide derivatives of these two series. In this work, we focus on NdW_{10} (**11**), whose energy level scheme is also plotted in Figure 3. As can be observed, the theoretical calculations describe a ground state with 95% of contribution of M_J = ±5/2, which is very similar to that of the mononuclear SMM YbW_{22}. This feature encouraged us to synthesize and magnetically characterize this new compound.

Magnetic Properties of NdW_{10}. From the energy level scheme and the contributions to the wave functions of NdW_{10} (illustrated in Figure 3), we calculate the temperature dependence of χT. The results are plotted in Figure 4 in comparison with the experimental results. As can be observed, an almost perfect agreement is found between the prediction and the experiment, demonstrating the usefulness of this strategy for the directed synthesis of new nanomagnets.

dx.doi.org/10.1021/ic501867d | Inorg. Chem. 2014, 53, 9976−9980

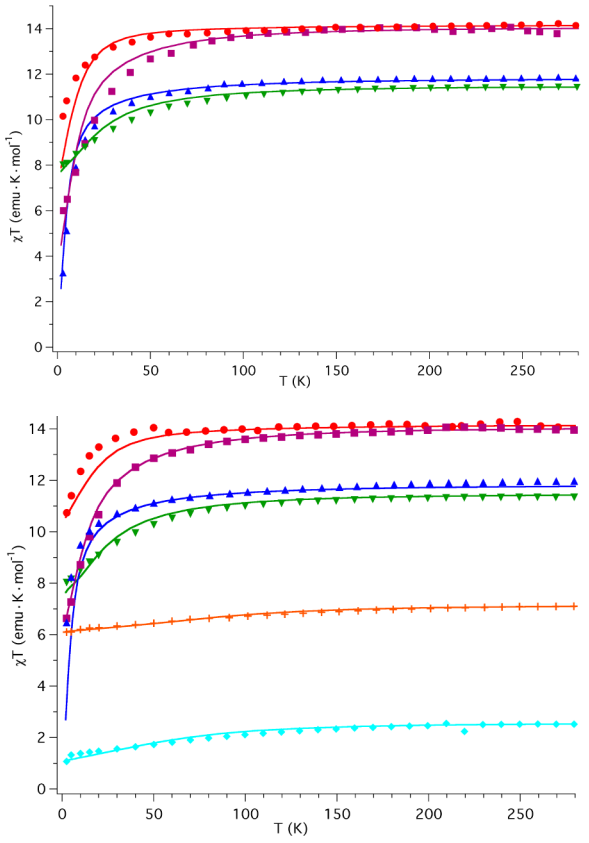

Figure 2. Fitting of the experimental χT product of the series of (top) $[Ln(W_5O_{18})_2]^{9-}$ and (bottom) $[Ln(\beta_2\text{-}SiW_{11}O_{39})_2]^{13-}$ (down) using the REC model: Dy (red ●), Ho (purple ■), Tb (blue ▲), Er (green ▼), Tm (red +), and Yb (light blue ◆). Markers give experimental data, and the solid lines give theoretical fits for Dy−Er and predictions for Tm and Yb.

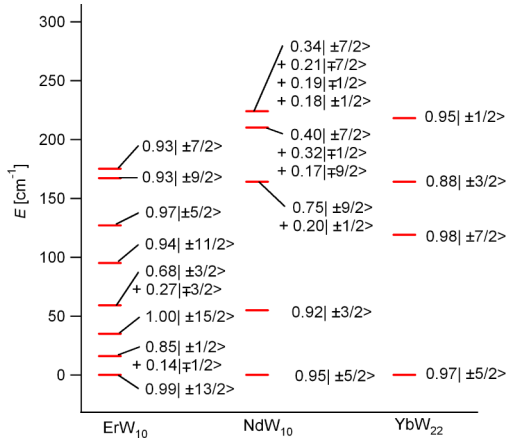

Figure 3. Energy level schemes and main M_J contributions for compounds **4**, **11**, and **10**. Note that all levels are Kramers doublets.

The ac magnetic properties reveal the typical features associated with the SMM behavior for a system with some mixture and thus the possibility of avoided hyperfine crossings and quantum tunneling (Figure 5). Thus, in the absence of a dc field there is a weak frequency-dependent signal in χ'' but no clear χ' signal. When an external field of 1000 Oe is applied, the system is taken beyond the hyperfine crossing region and as a result both χ' and χ'' show strong frequency dependences,

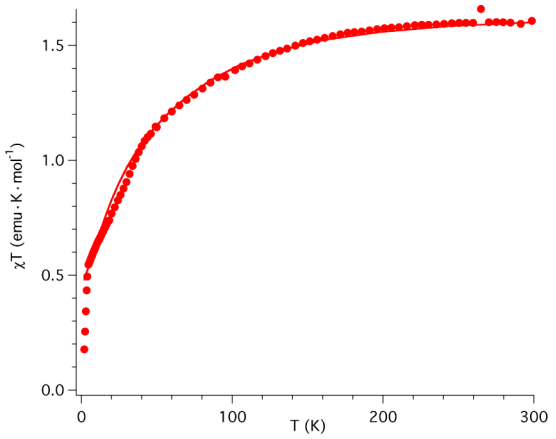

Figure 4. χT product of NdW_{10}. Circles give experimental data, and the solid line gives the theoretical prediction using the REC model.

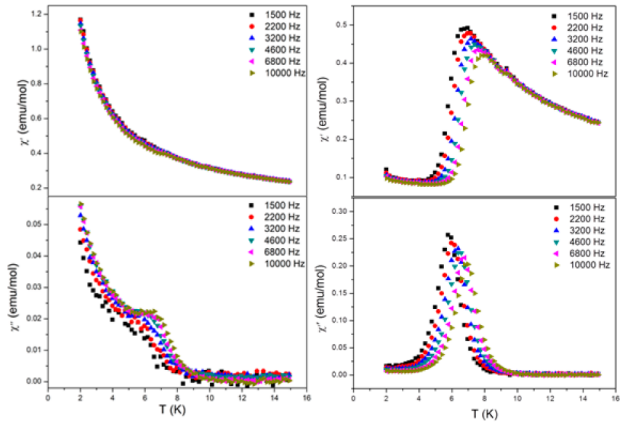

Figure 5. In-phase (top) and out-of-phase (bottom) dynamic susceptibility of **11**: without an external field (left) and with an applied field of 1000 Oe (right). The frequencies are shown in the legend.

which indicate the presence of a slow relaxation process involving an energy barrier for the reversal of the magnetization. Depending on the frequency of the applied ac field, χ' presents a maximum between 6.8 and 7.9 K, while χ'' has also a maximum between 5.9 and 6.9 K for 1500 and 10000 Hz, respectively (Figure 5, right). Analyses of the frequency dependence of the χ'' peaks through an Arrhenius plot allows the estimation of the magnetization−relaxation parameters in this system (Figure 6). Best fitting affords a barrier height (U_{eff}) of 51.4 cm^{-1} with a pre-exponential factor (τ_0) of 3.55×10^{-10} s. Given the good insulation of the Nd^{3+} ions provided by the diamagnetic polyoxowolframate framework (the shortest Nd−Nd distance is 11.221 Å), the slow relaxation process exhibited by the complex should be considered as a single-molecule property.

FINAL DISCUSSION

In this study, we have used two related families of lanthanoid POMs to estimate the parameters that describe the crystal field splitting caused by the oxo ligands in mononuclear f-element complexes. A qualitative analysis of these results has demonstrated that, while structural distortions will always introduce extradiagonal parameters in the CF Hamiltonian and therefore some degree of mixing in the ground-state wave functions, a rational design procedure can predict whether this

dx.doi.org/10.1021/ic501867d | Inorg. Chem. 2014, 53, 9976−9980

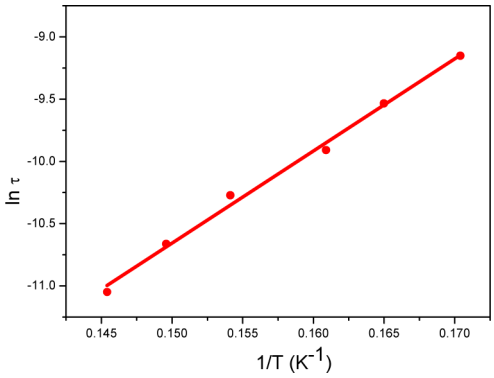

Figure 6. Relaxation-time fitting to the Arrhenius law in the 1500–10000 Hz interval for **11**.

will be a major effect for all metals or just a minor correction for most of them.

In Figure 7 we have included the two REC parameters associated with the oxygen donor atoms, O_W, in a general

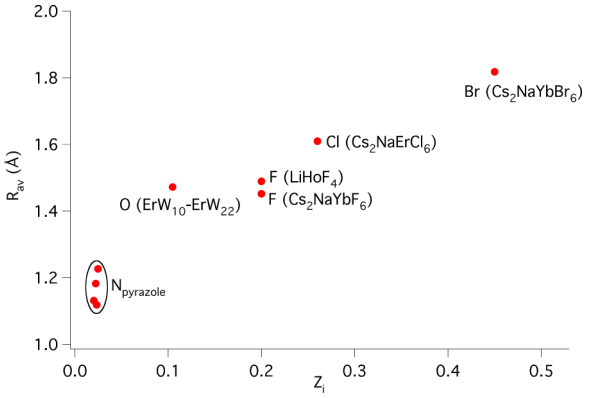

Figure 7. Average radius R_{av} and effective charge Z_i from the REC correction of different homoleptic compounds: nitrogenated ligands of the type bis-pyrazole or tris-pyrazole,[10e,22] oxygen atoms of the POM series LnW_{10} and LnW_{22}, and halide anions F^-, Cl^-, and Br^-.[20]

library that includes different donor atoms, obtained in previous works. In this comparison, the position of each ligand is illustrated in the plane defined by the effective charge and the average distance of said effective charge from the lanthanoid nucleus. This allows to quantify, for any given molecular geometry, the different relative tendency of each kind of ligand to produce CF splittings that are dominated by a simple double well (second order) or more complex energy level schemes typical of higher rank operators. Lower values of R_{av} lead to high-order effects (see eq 2 in the Supporting Information). This library may be very useful for the inexpensive rationalization and prediction of the magnetic properties of other SIMs, and the obtained CF parameters can be used as a starting point for further fittings of CF parameters when high-quality spectroscopic data are available. This will help to obtain a reliable description of spin eigenvectors that will permit researchers to deal with the potential application of these systems as spin qubits in quantum computing.[7,26]

In comparison with the ab initio approach, this method has the advantage of enabling intuitive comparisons between the different derivatives of the same family of compounds and the extrapolation of the crystal field effects of each particular kind of ligand. At present, the most important limitation of this *semiempirical* model is relying on susceptibility data, but ongoing studies, which take advantage of spectroscopic information, will enhance the accuracy of the parameters in the library. In a second step, for a full theoretical description of the CF splitting and the obtention of phenomenological CF parameters of a rare-earth compound, the full $4f^N$ configuration, the J–J mixing, and the configuration interaction (CI) should be taken into account, using the calculated CF parameters by the REC model as starting values. The solution to this open problem would be the combination of an inexpensive CF model, which allows the prediction of new derivatives, with sophisticated spectroscopic and single-crystal measurements to be made a posteriori, and finally, the fitting of phenomenological CF parameters, using a full approach, describing all the observables of the system with accuracy.

The predictive power of this *semiempirical* effective CF approach has been illustrated in this work. First, the REC parameters obtained for the oxo ligand from the χT product fit of **1**–**8** have been used to predict the χT vs T behavior of compounds **9** and **10**, obtaining a perfect match with the experimental data (Figure 2b, bottom). Second, in a further step we have predicted that, according to the previously reported crystal structure,[22] the Nd derivative of the LnW_{10} series should behave as a SMM. The Ising-type ground state and the χT theoretical prediction were confirmed experimentally, showing an excellent agreement between the predicted magnetic susceptibility curve and the experiment. In fact, an effective barrier of 51.4 cm^{-1} under an applied field of 1000 Oe was obtained for this POM derivative, which represents the second example of a neodymium-based SIM. These results indicate the power of a rational design strategy to broaden the SIM family, where the vast majority of SIMs are based on Dy^{3+}, to the early lanthanides, which still remain a mostly unexplored region in molecular magnetism.

■ ASSOCIATED CONTENT

Supporting Information

Text, figures, tables, and a CIF file giving the theoretical model, details of the synthesis and X-ray crystal structure determination of **11**, energy level schemes and ground state descriptions of **1**–**4** and **5**–**10**, and the IR spectrum and crystallographic data for **11**. This material is available free of charge via the Internet at http://pubs.acs.org.

■ AUTHOR INFORMATION

Corresponding Authors

*E-mail for E.C.: eugenio.coronado@uv.es.
*E-mail for A.G.-A.: alejandro.gaita@uv.es.

Notes

The authors declare no competing financial interest.

■ ACKNOWLEDGMENTS

The present work has been funded by the EU (Project ELFOS and ERC Advanced Grant SPINMOL), the Spanish MINECO (grants MAT2011-22785 and the CONSOLIDER project on Molecular Nanoscience CSD 2007-00010), and the Generalitat Valenciana (Prometeo and ISIC Programmes of excellence). A.G.-A. acknowledges funding by the MINECO (Ramón y Cajal contract). J.J.B. thanks the Spanish MINECO for an FPU predoctoral grant.

REFERENCES

(1) Sorace, L.; Benelli, C.; Gatteschi, D. *Chem. Soc. Rev.* **2011**, *40*, 3092−3104.

(2) Ishikawa, N.; Sugita, M.; Ishikawa, T.; Koshihara, S. Y.; Kaizu, Y. *J. Am. Chem. Soc.* **2003**, *125*, 8694−8695.

(3) AlDamen, M. A.; Clemente-Juan, J. M.; Coronado, E.; Martí-Gastaldo, C.; Gaita-Ariño, A. *J. Am. Chem. Soc.* **2008**, *130*, 8874−8875.

(4) (a) Rinehart, J. D.; Long, J. R. *Chem. Sci.* **2011**, *2*, 2078−2085. (b) Baldoví, J. J.; Cardona-Serra, S.; Clemente-Juan, J. M.; Coronado, E.; Gaita-Ariño, A. *Inorg. Chem.* **2012**, *51*, 12565−12574.

(5) AlDamen, M. A.; Cardona-Serra, S.; Clemente-Juan, J. M.; Coronado, E.; Gaita-Ariño, A.; Martí-Gastaldo, C.; Luis, F.; Montero, O. *Inorg. Chem.* **2009**, *48*, 3467−3479.

(6) Clemente-Juan, J. M.; Coronado, E.; Gaita-Ariño, A. *Chem. Soc. Rev.* **2012**, *41*, 7464−7578.

(7) (a) Stamp, P. C. E.; Gaita-Ariño, A. *J. Mater. Chem.* **2009**, *19*, 1718−1730. (b) Baldoví, J. J.; Cardona-Serra, S.; Clemente-Juan, J. M.; Coronado, E.; Gaita-Ariño, A.; Prima-García, H. *Chem. Commun.* **2013**, *49*, 8922−8924.

(8) (a) Freedman, D. E.; Harman, W. H.; Harris, T. D.; Long, G. J.; Chang, C. J.; Long, J. R. *J. Am. Chem. Soc.* **2010**, *132*, 1224−1225. (b) Harman, W. H.; Harris, T. D.; Freedman, D. E.; Fong, H.; Chang, A.; Rinehart, J. D.; Ozarowski, A.; Sougrati, M. T.; Grandjean, F.; Long, G. J.; Long, J. R.; Chang, C. J. *J. Am. Chem. Soc.* **2010**, *132*, 18115−181126. (c) Lin, P.-H.; Smythe, N. C.; Gorelsky, S. I.; Maguire, S.; Henson, N. J.; Korobkov, I.; Scott, B. L.; Gordon, J. C.; Baker, R. T.; Murugesu, M. *J. Am. Chem. Soc.* **2011**, *133*, 15806−15809. (d) Weismann, D.; Sun, Y.; Lan, Y.; Wolmershäuser, G.; Powell, A. K.; Sitzmann, H. *Chem. Eur. J.* **2011**, *17*, 4700−4704. (e) Atanasov, M.; Zadrozny, J. M.; Long, J. R.; Neese, F. *Chem. Sci.* **2013**, *4*, 139−156. (f) Zadrozny, J. M.; Atanasov, M.; Bryan, A. M.; Lin, C. Y.; Rekken, B. D.; Power, P. P.; Neese, F.; Long, J. R. *Chem. Sci.* **2013**, *4*, 125−138. (g) Mossin, S.; Tran, B. L.; Adhikari, D.; Pink, M.; Heinemann, F. W.; Sutter, J.; Szilagyi, R. K.; Meyer, K.; Mindiola, D. J. *J. Am. Chem. Soc.* **2012**, *134*, 13651−13661. (h) Zadrozny, J. M.; Long, J. R. *J. Am. Chem. Soc.* **2011**, *133*, 20732−20734. (i) Jurca, T.; Farghal, A.; Lin, P.-H.; Korobkov, I.; Murugesu, M.; Richeson, D. S. *J. Am. Chem. Soc.* **2011**, *133*, 15814−15817. (j) Zadrozny, J. M.; Liu, J.; Piro, N. A.; Chang, C. J.; Hill, S.; Long, J. R. *Chem. Commun.* **2012**, *48*, 3927−3929. (k) Graham, M. J.; Zadrozny, J. M.; Shiddiq, M.; Anderson, J. S.; Fataftah, M. S.; Hill, S.; Freedman, D. E. *J. Am. Chem. Soc.* **2014**, *136*, 7623−7626.

(9) (a) Luis, F.; Martínez-Pérez, M. J.; Montero, O.; Coronado, E.; Cardona-Serra, S.; Martí-Gastaldo, C.; Clemente-Juan, J. M.; Sesé, J.; Drung, D.; Schurig, T. *Phys. Rev. B* **2010**, *82*, 060403. (b) Martínez-Pérez, M. J.; Cardona-Serra, S.; Schlegel, C.; Moro, F.; Alonso, P. J.; Prima-García, H.; Clemente-Juan, J. M.; Evangelisti, M.; Gaita-Ariño, A.; Sesé, J.; van Slageren, J.; Coronado, E.; Luis, F. *Phys. Rev. Lett.* **2012**, *108*, 247213. (c) Jiang, S.; Wang, B.; Sun, H.; Wang, Z.; Gao, S. *J. Am. Chem. Soc.* **2011**, *133*, 4730−4733. (d) Jiang, S.; Wang, B.; Su, G.; Wang, Z.; Gao, S. *Angew. Chem., Int. Ed.* **2010**, *49*, 7448−7451. (e) Car, P. E.; Perfetti, M.; Mannini, M.; Favre, A.; Caneschi, A.; Sessoli, R. *Chem. Commun.* **2011**, *47*, 3751−3753. (f) Cucinotta, G.; Perfetti, M.; Luzon, J.; Etienne, M.; Carr, P. E.; Caneschi, A.; Calvez, G.; Bernot, K.; Sessoli, R. *Angew. Chem.* **2012**, *51*, 1606−1610.

(10) (a) Rinehart, J. D.; Long, J. R. *J. Am. Chem. Soc.* **2009**, *131*, 12558. (b) Rinehart, J. D.; Meihaus, K. R.; Long, J. R. *J. Am. Chem. Soc.* **2010**, *132*, 7572−7573. (c) Antunes, M. A.; Pereira, L. C. J.; Santos, I. C.; Mazzanti, M.; Marçalo, J.; Almeida, M. *Inorg. Chem.* **2011**, *50*, 9915−9917. (d) Coutinho, J. T.; Antunes, M. A.; Pereira, L. C. J.; Bolvin, H.; Marçalo, J.; Mazzanti, M.; Almeida, M. *Dalton Trans.* **2012**, *41*, 13568−13571. (e) Baldoví, J. J.; Cardona-Serra, S.; Clemente-Juan, J. M.; Coronado, E.; Gaita-Ariño, A. *Chem. Sci.* **2013**, *4*, 938−946. (f) Moro, F.; Mills, D. P.; Liddle, S. T.; van Slageren, J. *Angew. Chem., Int. Ed.* **2013**, *52*, 3430−3433. (g) Coutinho, J. T.; Antunes, M. A.; Pereira, L. C. J.; Marçalo, J.; Almeida, M. *Chem. Commun.* **2014**, *50*, 10262. (h) Meihaus, K. R.; Minasian, S. G.; Lukens, W. W.; Kozimor, S. A.; Shuh, D. K.; Tyliszczak, T.; Long, J. R. *J. Am. Chem. Soc.* **2014**, *136*, 6056−6068. (i) Mougel, V.; Chatelain, L.; Hermle, J.; Caciuffo, R.; Colineau, E.; Tuna, F.; Magnani, N.; de Geyer, A.; Pécaut, J.; Mazzanti, M. *Angew. Chem.* **2013**, *53*, 819−823.

(11) Duan, C. K.; Tanner, P. A. *J. Phys. Chem. A* **2010**, *114*, 6055−6062.

(12) (a) Batchelor, L. J.; Cimatti, I.; Guillot, R.; Tuna, F.; Wernsdorfer, W.; Ungur, L.; Chibotaru, L. F.; Campbell, V. E.; Mallah, T. *Dalton Trans.* **2014**, *43*, 12146−12149. (b) Bernot, K.; Luzón, J.; Bogani, L.; Etienne, M.; Sangregorio, C.; Shanmugam, M.; Caneschi, A.; Sessoli, R.; Gatteschi, D. *J. Am. Chem. Soc.* **2009**, *131*, 5573−5579. (c) Chilton, N. F.; Collison, D.; McInnes, E. J. L.; Winpenny, R. E. P.; Soncini, A. *Nat. Commun.* **2013**, *4*, 2551. (d) Marx, R.; Moro, F.; Dörfel, M.; Ungur, L.; Waters, M.; Jiang, S. D.; Orlita, M.; Taylor, J.; Frey, W.; Chibotaru, L. F.; van Slageren, J. *Chem. Sci.* **2014**, *5*, 3287−3293.

(13) Pedersen, K. S.; Ungur, L.; Sigrist, M.; Sundt, A.; Schau-Magnussen, M.; Vieru, V.; Mutka, H.; Rols, S.; Weihe, H.; Waldmann, O.; Chibotaru, L. F.; Bendix, J.; Dreiser, J. *Chem. Sci.* **2014**, *5*, 1650−1660.

(14) van Leusen, J.; Speldrich, M.; Schilder, H.; Kögerler, P. Submitted for publication.

(15) García, D.; Faucher, M. In *Handbook of the Physics and Chemistry of Rare Earths*; Gschneider, K. A., Jr., Eyring, L., Eds.; North-Holland: Amsterdam, 1995; Vol. *21*, Chapter 144.

(16) Jørgensen, C. K.; Pappalardo, R.; Schmidtke, H. B. *J. Chem. Phys.* **1963**, *39*, 1422−1430.

(17) Newman, D. J. *Adv. Phys.* **1971**, *20*, 197−256.

(18) Morrison, C. A. *Lectures on Crystal Field Theory HDL-SR-82-2 Report*, 1982.

(19) Malta, O. L. *Chem. Phys. Lett.* **1982**, *87*, 27−29.

(20) Baldoví, J. J.; Borrás-Almenar, J. J.; Clemente-Juan, J. M.; Coronado, E.; Gaita-Ariño, A. *Dalton Trans.* **2012**, *41*, 13705−13710.

(21) Baldoví, J. J.; Cardona-Serra, S.; Clemente-Juan, J. M.; Coronado, E.; Gaita-Ariño, A.; Palii, A. *J. Comput. Chem.* **2013**, *34*, 1961−1967.

(22) Baldoví, J. J.; Clemente-Juan, J. M.; Coronado, E.; Gaita-Ariño, A. *Polyhedron* **2013**, *66*, 39−42.

(23) Görller-Walrand, C.; Binnemans, K.. In *Handbook of the Physics and Chemistry of Rare Earths*; Gschneider, K. A., Jr., Eyring, L., Eds.; North-Holland: Amsterdam, 1996; Vol. *23*, pp 121−183.

(24) Rinehart, J. D.; Long, J. R. *Dalton Trans.* **2012**, *41*, 13572−13574.

(25) Hill, S.; Coronado, E. Manuscript in preparation.

(26) (a) Ardavan, A.; Blundell, S. J. *J. Mater. Chem.* **2009**, *19*, 1754−1760. (b) Troiani, F.; Affronte, M. *Chem. Soc. Rev.* **2011**, *40*, 3119−3129.